Non-contrast-enhanced MR angiography of the thoracic central veins

Andrew Nicholas Priest[1], Gavin Low[1], Martin John Graves[1], and David John Lomas[1]
[1]*Radiology, Addenbrooke's Hospital and University of Cambridge, Cambridge, United Kingdom*

Target audience Physicists and clinicians interested in vascular imaging

Purpose

Imaging of the central thoracic veins can allow assessment of patients with central venous obstruction or restricted venous access (including identification of possible venous access points). However contrast agent administration is difficult in the latter group (by definition), and may also have risks given that many of these patients have impaired renal function. A non-invasive method for imaging central veins, without administration of contrast agent, would therefore be valuable, but must address the dual problems of respiratory and cardiac motion. The aim of this work was to adapt, optimise and evaluate the feasibility of a recently-developed non-contrast-enhanced MR angiography (NCE-MRA) methods[1] for application in the thorax.

Methods

Following ethical approval and informed consent, 6 healthy volunteers were imaged at 1.5 T (Discovery MR450, GE Healthcare, Waukesha, WI) using an 8-channel cardiac array coil. The NCE-MRA method used subtraction of bright- and dark-blood images to form an angiogram showing flowing blood in the central thoracic vessels but with most static tissue signal removed[1]. The bright- and dark-blood image acquisitions were interleaved to minimise the impact of bulk motion, and used the pulse sequence shown schematically in Fig. 1. Flow suppression was achieved using 2 consecutive velocity-selective iMSDE modules[2], which were placed at the time of approximately peak venous flow within the cardiac cycle (typically ~200ms after ECG trigger) and had differently oriented motion suppression gradients[3] (in this case +x,+y and +x,-y) with duration 4 ms, amplitude 6 mT/m. The image readout (segmented 3D balanced SSFP) was placed during the systolic cardiac rest period to minimise the impact of cardiac motion and used the following parameters: coronal orientation, flip angle 65°, TE/TR=1.4/3.1 ms, acquisition matrix 256×256, FoV 40 cm, 20 slices of 4 mm, 1 Nex, ASSET factor 2, 3 segments per k-space plane, segment TR 2 heartbeats, 10 sinusoidally increasing dummy acquisitions, segment duration 131ms. A paired centric k-space order was used to avoid phase-encode eddy-current artifacts[4]. Spatial saturation bands were used to remove residual phase-wrap in the slice-selection direction. Navigator gating (without slab-tracking, acceptance window 3–4 mm) was used to compensate for respiratory motion; the navigator was acquired before the iMSDE modules to avoid them interfering with the navigator signal. The total acquisition time was 240 heartbeats (assuming 100% navigator efficiency).

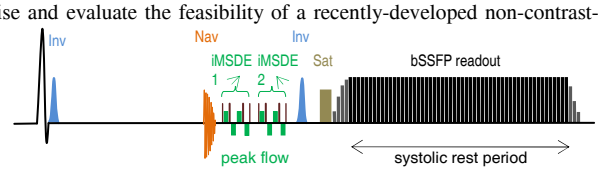

Fig. 1: schematic pulse sequence, including 2 inversion pulses, navigator, two iMSDE modules, saturation and bSSFP readout.

Additionally breath-hold acquisitions were acquired using acquisition matrix 256×192, 0.5 Nex, 12–14 slices of 5–6 mm, 1 segment per k-space plane, segment TR 1 heartbeat, other parameters as above (segment duration 196 ms, total acquisition time 24–26 heartbeats).

Optionally, a dual inversion-recovery (DIR) method was used to suppress the fat signal: this consisted of one inversion pulse immediately after the cardiac trigger and another after the iMSDE modules. The second inversion, occurring around the time of the fat null point, allowed re-inversion of the long-T1 blood magnetisation to avoid substantial blood signal loss. DIR was compared with spectral fat suppression and with no fat suppression.

The images were assessed qualitatively by an experienced radiologist, viewing all slices and focussing on the major veins: superior vena cava (SVC), innominate and subclavian veins. The image quality, artefact levels and background signal were rated for each image on 5-point Likert scales (1–5, 1 best, 4–5 diagnostically limited).

Results

Fig. 2 shows images for each acquired method in an example volunteer. Fig. 3 shows a stacked-bar plot of the qualitative scores (dark bars are best, length = number of scores). Both image quality and artifact scores were higher for the navigated sequences, with DIR the best-scoring, and poorer (non-diagnostic) for the breath-hold sequences. Background levels were better with DIR or spectral fat suppression than with no fat suppression.

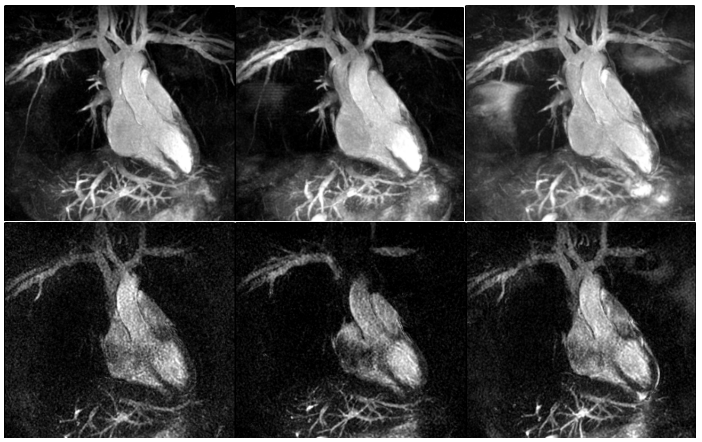

Fig. 2: Example MIPs of the subtraction angiograms using DIR (left), spectral fat suppression (center), and no fat suppression (right); upper images are navigator-gated, lower images breath-hold.

Discussion

The free-breathing navigator-gated approach appears to be give good image quality and motion compensation. However, the breath-hold acquisitions were unsatisfactory due to the measures taken to shorten the acquisition time, in particular: (a) the reduced segment TR leading to inadequate signal recovery, especially with the DIR approach; (b) the longer segment duration, which exceeds the cardiac rest period leading to motion artifact; and possibly (c) the use of partial Fourier reconstruction especially in regions of poor shim.

Given the high amplitude fat signal on the source images, subtraction alone often led to poor background signal suppression. Spectral fat suppression reduced background signal levels, but sometimes gave poor image quality—especially signal voids in the SVC which we speculate are unintended suppression of water instead of fat due to off-resonance effects. By contrast the DIR approach allowed good suppression of background signals with only modest signal loss in the vessels.

The overall best approach, combining navigator-gating and DIR, gave mostly good quality images and had the best or joint best image quality in all but one subject. In some cases, the image quality was reduced by off-resonance effects such as bSSFP-related banding artifacts: future modifications will therefore focus initially on improving the shim and/or the robustness of the image readout.

Variants of the navigator-gated method could also be useful for NCE-MRA of other thoracic or abdominal vessels including the major thoracic arteries, the hepatic and splenic vessels, which are also well visualised on these images.

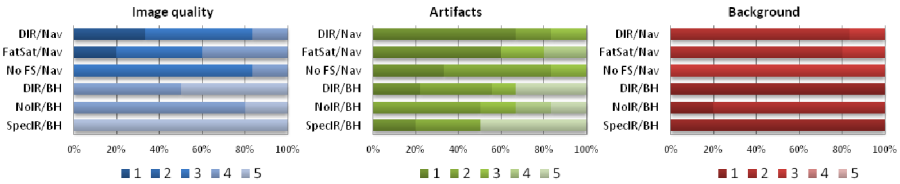

Fig. 3: Stacked-bar plots of the scores for image quality, artifacts and background signal. Scores range from 1–5 with 1 (darkest) the best score and 5 (lightest) the worst score, and relate to the three different fat suppression methods with navigator (top 3 bars) or breath-hold (bottom 3).

Conclusion

Imaging of the thoracic central veins is feasible using a novel navigated NCE-MRA method; the best image quality was found by using DIR to suppress unwanted background signals.

References

1. Priest AN, Graves MJ, Lomas DJ. Non-contrast-enhanced vascular magnetic resonance imaging using flow-dependent preparation with subtraction. Magn Reson Med. 2012;67(3):628–637.

2. Wang J, Yarnykh VL, Yuan C. Enhanced image quality in black-blood MRI using the improved motion-sensitized driven-equilibrium (iMSDE) sequence. J Magn Reson Imaging. 2010;31(5):1256–63.

3. Fan Z, Hodnett PA, Davarpanah AH, et al. Noncontrast magnetic resonance angiography of the hand: improved arterial conspicuity by multidirectional flow-sensitive dephasing magnetization preparation in 3D balanced steady-state free precession imaging. Invest Radiol. 2011;46(8):515-23.

4. Bieri O, Markl M, Scheffler K. Analysis and compensation of eddy currents in balanced SSFP. Magn Reson Med. 2005;54(1):129-37.